Journal of Alloys and Compounds 509 (2011) 1870–1873

Contents lists available at ScienceDirect

Journal of Alloys and Compounds

journal homepage: www.elsevier.com/locate/jallcom

Synthesis and luminescent properties of Eu^{2+} doped $BaZn_2Si_2O_7$ phosphors by combustion-assisted synthesis method

Shan-shan Yao, Li-hong Xue*, You-wei Yan

State Key Laboratory of Materials Processing and Die & Mould Technology, College of Materials Science and Engineering, Huazhong University of Science & Technology, Wuhan 430074, Hubei, PR China

ARTICLE INFO

Article history:
Received 23 June 2010
Received in revised form 9 October 2010
Accepted 22 October 2010
Available online 29 October 2010

Keywords:
Optical materials
Chemical synthesis
Optical properties
Luminescence

ABSTRACT

A green emitting phosphor of the orthorhombic $BaZn_2Si_2O_7:Eu^{2+}$ was prepared by the combustion-assisted synthesis method and an efficient green emission under near-ultraviolet was observed. The luminescence and crystallinity were investigated by using luminescence spectrometry, X-ray diffractometry (XRD). The emission spectrum shows a single intensive band centered at 522 nm, which corresponds to the $4f6^5d^1 \rightarrow 4f^7$ transition of Eu^{2+}. The excitation spectrum is a broad extending from 260 to 465 nm, which matches the mission of ultraviolet light-emitting diodes (UV-LEDs). The critical quenching concentration of Eu^{2+} in $BaZn_2Si_2O_7:Eu^{2+}$ phosphor is about 0.05. The corresponding concentration quenching mechanism is verified to be a dipole–dipole interaction. The chromaticity coordinates were obtained from the luminescence emission spectrum. The results indicate that $BaZn_2Si_2O_7:Eu^{2+}$ can be potentially useful as a UV radiation-converting phosphor for white light-emitting diodes (LEDs).

1. Introduction

White light-emitting diodes (LEDs) offer benefits such as a high luminous efficiency, energy saving, maintenance and environmental protection, therefore, they are tripped to be the next generation solid-state lighting, in the replacement of conventional incandescent and fluorescent lamps [1]. The light-conversion phosphors for solid-state lighting have attracted much attention in recent years [2–11]. The most common method to generate the white LEDs for solid-state lighting is to combine a blue LED with a yellow phosphor YAG:Ce^{3+} [12,13]. However, this strategy faces serious problems of poor color rendering index, narrow visible range, and high color temperature. As an alternative, a novel approach has been suggested, the use of ultraviolet (UV) excitation to generate white LED. Recently, white LEDs fabricated by red/green/blue tricolor phosphors with near-UV Ga(In)N chips have been considered as the most efficient method because n-UV lights have little effect on the color quality [13]. In this work, the potential green phosphors with high emission efficiency under the excitation of near UV light were studied.

Silicates are excellent hosts for ultraviolet LEDs due to their high chemical–physical stability and various crystal structures. The emission color of Eu^{2+}-activated silicates can be controlled by changing the crystal field in the host, which due to the fact the emission of Eu^{2+} ion could vary from ultraviolet to red depending on the host lattice because of its parity-allowed 4f–5d transition [14–19]. Recently, phosphate has become an important luminescent material because of its excellent thermal and charge stabilization [20]. In this paper, the $BaZn_2Si_2O_7:Eu^{2+}$ green-emitting phosphor was synthesized by combustion-assisted synthesis method and its luminescent properties were also investigated.

2. Experimental

2.1. Sample preparation

Powder samples with the general formula $(Ba_{1-x}, Eu_x)Zn_2Si_2O_7$ (x = 0–0.09) phosphor were prepared by the combustion-assisted synthesis method. The starting reagents were $Ba(NO_3)_2$ (AR), $Zn(NO_3)_2{\cdot}6H_2O$ (AR), $Si(OC_2H_5)_4$ (AR), Eu_2O_3 (99.99%). NH_2CONH_2 was added as a fuel and small quantities of H_3BO_3 as a flux, respectively. From the literature [21], we find that $Si(OC_2H_5)_4$ (AR) was used as a silica source for combustion synthesis. For the calculation of oxidizer to fuel ratio, the elements are assigned formal valences as follows: Ba = +2, Zn = +2, Eu = +3, Si = +4, B = +3, C = +4, H = +1, O = −2 and N = 0. Accordingly, the oxidizer and fuel values for various reactants are given as below:

$$\underset{-9.5}{0.95Ba(NO_3)_2} + \underset{-20}{2Zn(NO_3)_2} + \underset{-0.75}{Eu(NO_3)_3} + \underset{0}{2Si(OH)_4} + \underset{0}{H_3BO_3} + \underset{+6}{CO(NH_2)_2}$$

For complete combustion, the oxidizer/fuel ratio should be equal to 1. Thus, the molar ratio of the reactants taken is 0.95:2:0.05:2:0.06:5 of $Ba(NO_3)_2$:$Zn(NO_3)_2$:$Eu(NO_3)_3$:$Si(OH)_4$:H_3BO_3:$CO(NH_2)_2$. The appropriate amounts of reactants were mixed in a glass beaker to get a clear solution. Then the mixture solution was introduced into a muffle furnace preheated to 600 °C. Within a few minutes, the solution boiled and was ignited to produce a self-propagating flame. The product was postannealed in reducing reductive atmosphere at 1100 °C for 5 h.

* Corresponding author. Tel.: +86 27 87543876; fax: +86 27 87541922.
E-mail address: xuelh@mail.hust.edu.cn (L.-h. Xue).

0925-8388/$ – see front matter © 2010 Elsevier B.V. All rights reserved.
doi:10.1016/j.jallcom.2010.10.076

2.2. Characterization samples

The synthesized phosphors were ground to powder and passed through a 200 mesh sieve prior to the characterization. The crystal phase of the synthesized powders prepared in the process was characterized by X-ray powder diffraction using an X′ Pert PRO X-ray diffractometer having a Cu Kα radiation (λ = 1.5406 Å) at 40 kV tube voltage and 40 mA tube current. The XRD patterns were collected in the range of $10^\circ \le 2\theta \le 90^\circ$. The emission spectrum was measured on a RF-5301 fluorescence spectrophotometer equipped with a xenon discharge lamp as an excitation source. The excitation and emission slits were set to 3.0 nm. All the above measurements were taken at room temperature.

The chromaticity coordinates were obtained according to the Commission International de l'Eclairage (CIE) using a Spectra Lux Software v.2.0 Beta [22,23].

3. Results and discussion

3.1. Crystal structure and phase formation

The crystal structure of $BaZn_2Si_2O_7$ is composed of a tetrahedron framework, $[Zn_2Si_2O_7]$, and isolated barium atoms. Two silicon tetrahedral are connected by sharing an oxygen, forming a di-silicate group Si_2O_7. The di-silicate groups further share corner with the $[ZnO_4]$, forming a three-dimensional framework [24]. All of the barium atoms are located in the channel and coordinated by oxygen atoms in both the structures (Fig. 1).

XRD patterns of $BaZn_2Si_2O_7$ and $Ba_{1-x}Zn_2Si_2O_7{:}Eu_x^{2+}$ samples postannealed at 1100 °C for 5 h are shown in Fig. 2. There are no observable differences between these diffraction patterns, indicating that the little amount of doped rare-earth ions has almost no effect on the $BaZn_2Si_2O_7$ crystalline structure. The pure phase of $BaZn_2Si_2O_7$ has formed in these samples. The diffraction peak positions are well matched with that in the literature (orthorhombic crystal system, space group $Ccm2_1$, $a = 7.6199$ Å, $b = 13.0265$ Å, $c = 6.7374$ Å, $\alpha = \beta = \gamma = 90^\circ$) [24]. In this work, the structure of $BaZn_2Si_2O_7$ with space group $Ccm2_1$ was taken as the starting model for the synthesized phosphors.

The lattice parameters listed in Table 1 shows that there is good agreement between the literature and the prepared $BaZn_2Si_2O_7$ and $Ba_{1-x}Zn_2Si_2O_7{:}Eu_x^{2+}$ ($x = 0.01$–0.09) samples values, suggesting that the method starting from the silicates is successfully applied here. Meanwhile, it is clear that the Eu^{2+} doping ions do not change the general structure.

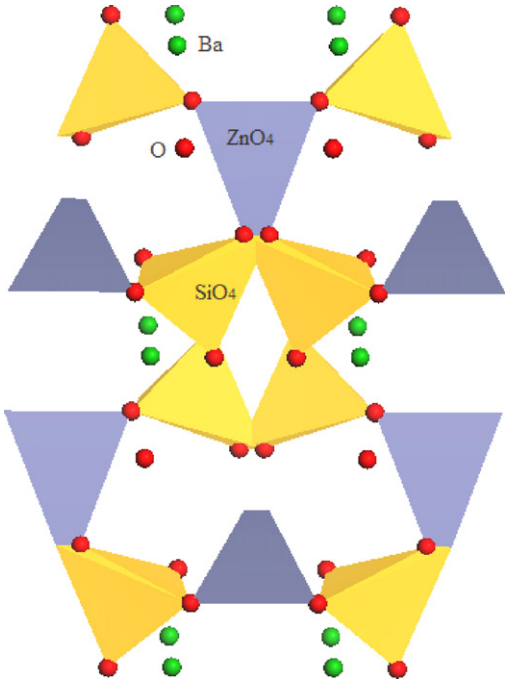

Fig. 1. Crystal structure of $BaZn_2Si_2O_7$.

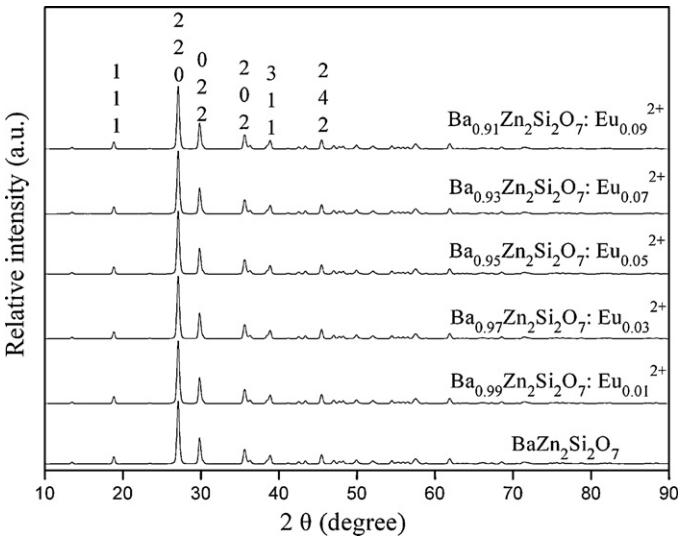

Fig. 2. X-ray diffraction patterns of $Ba_{1-x}Zn_2Si_2O_7{:}Eu_x^{2+}$ ($x = 0$, 0.01, 0.03, 0.05, 0.07, 0.09).

Table 1
Lattice parameters values of $Ba_{1-x}Zn_2Si_2O_7{:}Eu_x^{2+}$ ($x = 0$, 0.01, 0.03, 0.05, 0.07, 0.09) phosphors calculated from the XRD pattern.

Samples	a (Å)	b (Å)	c (Å)	V (Å^3)
$BaZn_2Si_2O_7$ (this work)	7.5485	13.1647	6.7342	669.2084
$Ba_{0.99}Zn_2Si_2O_7{:}Eu_{0.01}^{2+}$	7.5583	13.1004	6.7260	666.9855
$Ba_{0.97}Zn_2Si_2O_7{:}Eu_{0.03}^{2+}$	7.5575	13.1361	6.7278	667.0238
$Ba_{0.95}Zn_2Si_2O_7{:}Eu_{0.05}^{2+}$	7.5519	13.1157	6.7368	667.2640
$Ba_{0.93}Zn_2Si_2O_7{:}Eu_{0.07}^{2+}$	7.5450	13.0988	6.7388	667.9950
$Ba_{0.91}Zn_2Si_2O_7{:}Eu_{0.09}^{2+}$	7.5433	13.0850	6.7413	668.1354
Ref. [17]	7.6199	13.0265	6.7374	668.76

An acceptable percentage difference in ion radii between doped and substituted ions must not exceed 30% [25]. The calculations of the radius percentage difference (D_r) between the doped ions (Eu^{2+}) and possible substituted ions (Ba^{2+}, Zn^{2+}, Si^{4+}) in $BaZn_2Si_2O_7$ are summarized in Table 2. The values are based on the following formula:

$$D_r = \frac{R_m(CN) - R_d(CN)}{R_m(CN)} \quad (1)$$

where CN is the coordination number, $R_m(CN)$ is the radius of the host cation, and $R_d(CN)$ is the radius of the doped ion. We take the data of Eu^{2+} with $CN = 6$ as a responsible approximation [26]. The value of D_r between Eu^{2+} and Ba^{2+} on nine-coordinated sites are 24.93%, while D_r between Eu^{2+} and Zn^{2+} (or Si^{4+}) is −58.11% (or −192.50%). Obviously, the doping ions of Eu^{2+} will clearly substitute the barium sites.

Table 2
Ionic radii difference percentage (D_r) between matrix cations and doped ions.

Doped ions	$R_d(CN)$ (Å)	$D_r = [R_m(CN) - R_d(CN)]/R_m(CN)$ (%)		
		$R_{Ba}^{2+}(8) =$ 1.42 (Å)	$R_{Zn}^{2+}(6) =$ 0.74 (Å)	$R_{Si}^{4+}(6) =$ 0.40 (Å)
Eu^{2+}	1.17 (6) 1.30 (9)	24.93	−58.11	−192.50

CN stands for coordination number, R_m (CN) and R_d (CN) for the radii of matrix and doped cations, respectively, and the data of the effective ionic radii are from Ref. [27].

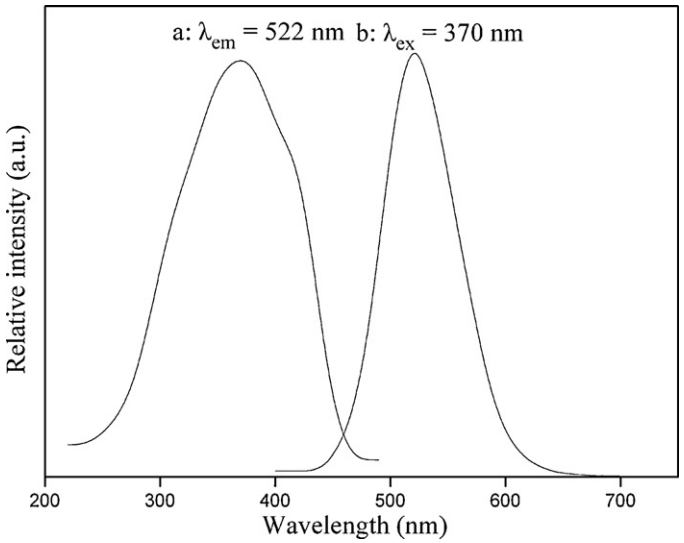

Fig. 3. The excitation (λ_{em} = 522 nm) and emission (λ_{ex} = 370 nm) spectra of $Ba_{0.95}Zn_2Si_2O_7:Eu_{0.05}{}^{2+}$.

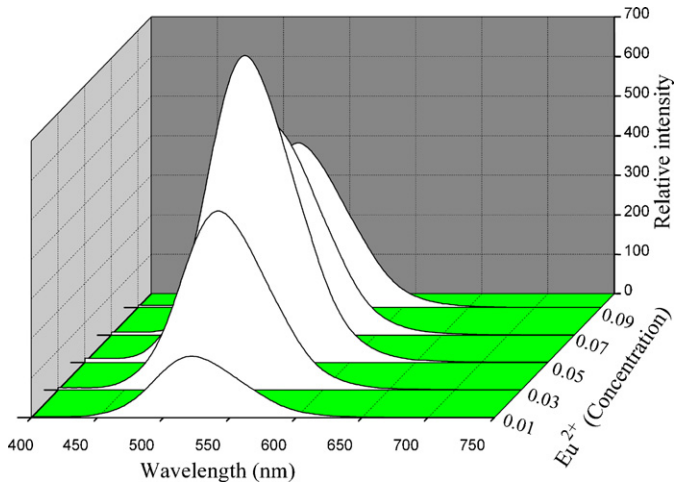

Fig. 4. Emission (λ_{ex} = 370 nm) intensity of $Ba_{1-x}Zn_2Si_2O_7:Eu_x{}^{2+}$ with different Eu^{2+} concentrations.

3.2. Luminescent properties

The emission and excitation spectra of $Ba_{0.95}Zn_2Si_2O_7:Eu_{0.05}{}^{2+}$ phosphor are presented in Fig. 3. With excitation wavelength of 370 nm, the emission spectrum exhibits a green band centering at 522 nm. It corresponds to the allowed f–d transition of Eu^{2+}. The 5d energy level of Eu^{2+} and the lower level of 4f state overlap, so the electron of 4f state can be excited to 5d state. The broad luminescence of Eu^{2+} is due to $4f^6 5d^1 \rightarrow 4f^7$ transitions, which is an allowed electrostatic dipole transition. However, the 5d state is easily affected by the crystal field, that is to say, different crystal fields can split the 5d state in different way. This makes Eu^{2+} emitting different wavelength light in different crystal fields and the emission spectrum can vary from the ultraviolet to the red region [28]. The codopant Eu^{2+} ions are substituted for the Ba^{2+} sites and are exposed to a strong crystal field, the excitation band of Eu^{2+} extends into the visible region. The main excitation peak is located at 370 nm, which indicates that the phosphor is very suitable for a color converter using UV light as the primary light source. It can be used as a green phosphor excited by UV-LED chip and mixed with other color emission phosphors to obtain white light.

A series of $Ba_{1-x}Zn_2Si_2O_7:Eu_x{}^{2+}$ phosphor with various Eu^{2+} concentration (x = 0.01–0.09) were prepared and the effect of doped Eu^{2+} concentration on the emission intensity was instigated. Emission intensity of $Ba_{1-x}Zn_2Si_2O_7:Eu_x{}^{2+}$ with different Eu^{2+} concentration is shown in Fig. 4. The positions of the emission peak are not influenced by the Eu^{2+} concentration. The emission intensity increases with increasing of Eu^{2+} concentration, and reaches the maximum at about 0.05. Concentration quenching occurs, when the Eu^{2+} concentration is beyond 0.05.

With respect to the mechanism of energy transfer in phosphors, Blasse has pointed out that the critical transfer distance (R_c) is approximately equal to twice the radius of a sphere with this volume [29]:

$$R_c \approx 2\left(\frac{3V}{4\pi x_c N}\right)^{1/3} \quad (2)$$

where x_c is the critical concentration, N is the number of cations in the unit cell and V is the volume of the unit cell. By taking the experimental and analytical values of V, N and x_c (667.2640 Å^3, 4, 0.05, respectively), the critical transfer distance of Eu^{2+} in $BaZn_2Si_2O_7$ phosphor is calculated to be about 18.54 Å.

Non-radiative energy transfer from a Eu^{2+} ion to another Eu^{2+} ion may occur by exchange interaction, radiation reabsorption or multipole–multipole interaction. Eu^{2+} is an isolated emission center in $BaZn_2Si_2O_7:Eu^{2+}$ phosphor. The $4f^7 \rightarrow 4f^6 5d^1$ transition of Eu^{2+} is allowed for exchange interactions and typical critical distances should be about 5 Å [30]. This indicates that the mechanism of exchange interaction plays no role in energy transfer between Eu^{2+} ions in $BaZn_2Si_2O_7:Eu^{2+}$ phosphor. The mechanism of radiation reabsorption comes into effect only when there is a broad overlap of the fluorescent spectra of the sensitizer and activator. In the view of the emission and excitation spectra of $BaZn_2Si_2O_7:Eu^{2+}$ phosphor, it is unlikely to occur in this case. Since the fluorescent mechanism of Eu^{2+} in $BaZn_2Si_2O_7:Eu^{2+}$ phosphor is the 4f→ 5d allowed electric-dipole transition, the process of energy transfer should be controlled by electric multipole–multipole interaction according to Dexter's theory [30]. Furthermore, according to the literature [31], a multipole–multipole interaction currently occurs when the distance between two ions is about 20.0 Å, which is in good agreement with our calculated value (18.54 Å). If the energy transfer occurs between the same sort of activators, the intensity of multipolar interaction can be determined based on the change of the emission intensity from the emitting level which has the multipolar interaction. The emission intensity (I) per activator ion follows the equation [32,33]:

$$\frac{I}{x} = K[1 + \beta(x)^{Q/3}]^{-1} \quad (3)$$

where x is the activator concentration; Q = 6, 8, 10 for dipole–dipole, dipole–quadrupole, quadrupole–quadrupole interactions, respectively; and K and β are constant for the same excitation conditions for a given host crystal.

The critical concentration of Eu^{2+} has been determined to be 0.05 mol. The dependence of the emission intensity of $BaZn_2Si_2O_7:Eu^{2+}$ phosphor excited at 370 nm as a function of the corresponding concentration of Eu^{2+} for concentration greater than the critical concentration is the determined. The plot of $\lg I/x_{Eu^{2+}}$ as a function of $\lg x_{Eu^{2+}}$ in $Ba_{1-x}Zn_2Si_2O_7:Eu_x{}^{2+}$ phosphors are shown in Fig. 5. It can be seen that the dependence of $\lg I/x_{Eu^{2+}}$ on $\lg x_{Eu^{2+}}$ is linear and the slope is −2.211. The value of Q can be calculated as 6.633, which is close to 6. This indicates that the dipole–dipole interaction is the concentration quenching mechanism of Eu^{2+} emission in the $BaZn_2Si_2O_7:Eu^{2+}$ phosphor.

Color purity can be visualized in the chromaticity diagram (Fig. 6) as blue, red, and green regions, using the emission color coordinates of the luminescent material. So, from the luminescence

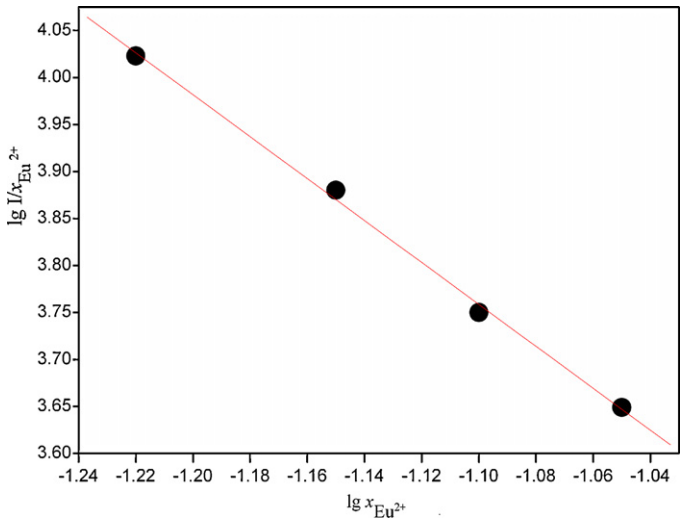

Fig. 5. Plot of $\lg I/x_{Eu^{2+}}$ as a function of $\lg x_{Eu^{2+}}$ in $Ba_{1-x}Zn_2Si_2O_7:Eu_x^{2+}$ phosphors (λ_{ex} = 370 nm).

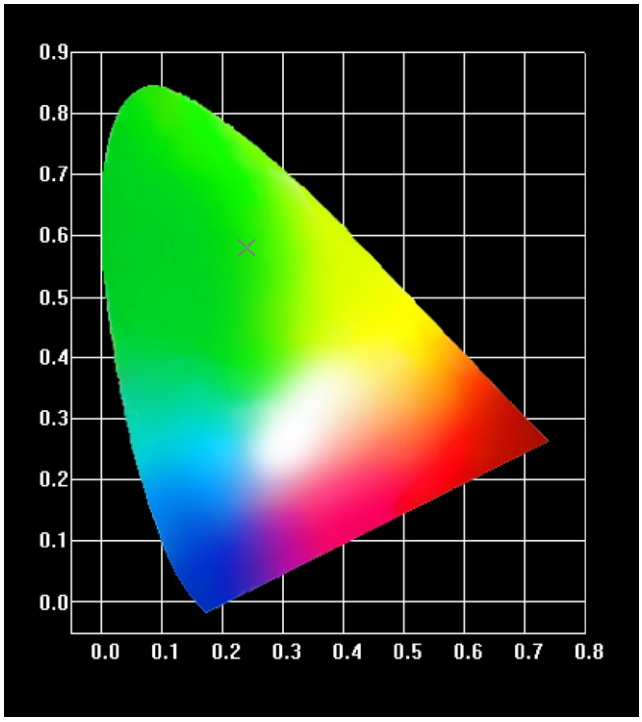

Fig. 6. Chromaticity coordinates from emission spectra of the $Ba_{0.95}Zn_2Si_2O_7:Eu_{0.05}^{2+}$.

emission spectra of $Ba_{0.95}Zn_2Si_2O_7:Eu_{0.05}^{2+}$ sample, we obtained the chromaticity diagrams with the aid of the Spectra Lux Software v.2.0 Beta [22]. For any given color there is one setting for each set of three numbers, *X*, *Y*, and *Z*, known as tristimulus values that will produce a match. Based on the emission spectra of $Ba_{0.95}Zn_2Si_2O_7:Eu_{0.05}^{2+}$ sample, the (*x*, *y*) color coordinates were determined with the following values (*x*, *y*) = (0.24, 0.58).

4. Conclusion

The orthorhombic $BaZn_2Si_2O_7:Eu^{2+}$ phosphors were synthesized by a combustion-assisted synthesis method and its luminescent properties were also investigated. With an increase in the Eu^{2+} concentration, quenching of the excitation energy occurs. The critical quenching concentration of Eu^{2+} in $BaZn_2Si_2O_7:Eu^{2+}$ phosphor is determined as 0.05 mol. The critical transfer distance is calculated as 18.54 Å. The mechanism of concentration quenching of $BaZn_2Si_2O_7:Eu^{2+}$ is determined to be the dipole–dipole interaction. Eu^{2+} ions only occupy Ba^{2+} sites and form one emission center at 522 nm. The CIE of the optimized sample was calculated (*x*, *y*) = (0.24, 0.58). The excitation spectrum couples well with the emission of UV-LED chips (350–410 nm). The results indicated that $BaZn_2Si_2O_7:Eu^{2+}$ is a potential green phosphor for UV-LEDs.

Acknowledgements

This work was supported by the Natural Science Foundation of China (No. 51002054), the Natural Science Foundation of Hubei Province of China (No. 2008CB252), the Fundamental Research Funds for the Central Universities (C2009Q012) and by the Scientific Research Foundation for the Returned Overseas Chinese Scholar, State Education Ministry.

References

[1] E.F. Schubert, J.K. Kim, Science 308 (2005) 1274–1278.
[2] Z.C. Wu, J. Liu, W.G. Hou, J. Xu, M.L. Gong, J. Alloys Compd. 498 (2010) 139–142.
[3] A. Xie, X.M. Yuan, F.X. Wang, Y. Shi, J. Li, L. Liu, Z.F. Mu, J. Alloys Compd. 501 (2010) 124–129.
[4] S.S. Yao, Y.Y. Li, L.H. Xue, Y.W. Yan, J. Alloys Compd. 491 (2010) 264–267.
[5] W.J. Park, M.K. Jung, S.M. Kang, T. Masaki, D.H. Yoon, J. Phys. Chem. Sol. 69 (2008) 1505–1508.
[6] Y.K. Kim, S. Choi, H.K. Jung, J. Lumin. 130 (2010) 60–64.
[7] J. Jeong, M. Jayasimahari, H.S. Lee, K. Jang, S.S. Yi, J.H. Jeong, C. Kim, Physica B 404 (2009) 2016–2019.
[8] H.Y. Chung, C.H. Lu, C.H. Hsu, J. Am. Ceram. Soc. 93 (2010) 1838–1841.
[9] C.F. Guo, Y. Xu, F. Lv, X. Ding, J. Alloys Compd. 497 (2010) L21–L24.
[10] S.S. Yao, Y.Y. Li, L.H. Xue, Y.W. Yan, Phys. Status Solidi A 207 (2010) 2164–2169.
[11] I.M. Nagpure, K.N. Shinde, V. Kumar, O.M. Ntwaeaborwa, S.J. Dhoble, H.C. Swart, J. Alloys Compd. 492 (2010) 384–388.
[12] S. Nakamura, S. Pearton, G. Fasol, The Blue Laser Diode, 2nd ed., Springer, Berlin, 2000.
[13] J.K. Sheu, S.J. Chang, C.H. Kuo, Y.K. Su, L.W. Wu, Y.C. Lin, W.C. Lai, J.M. Tsai, G.C. Chi, R.K. Wu, IEEE Photo. Technol. Lett. 15 (2003) 18–20.
[14] S.S. Yao, Y.Y. Li, L.H. Xue, Y.W. Yan., J. Am. Ceram. Soc., (2010) doi:10.1111/j.1551-2916.2010.03929.x.
[15] H. He, X.F. Song, R.L. Fu, Z.W. Pan, X.R. Zhao, Z.H. Deng, Y.G. Gao, J. Alloys Compd. 493 (2010) 401–405.
[16] H.Y. Wu, Y.H. Hu, Y.H. Wang, C.J. Fu, J. Alloys Compd. 497 (2010) 330–335.
[17] C.J. Fu, Y.H. Hu, Y.H. Wang, H.Y. Wu, X.J. Wang, J. Alloys Compd. 502 (2010) 423–428.
[18] H. Kamioka, T. Yamaguchi, M. Hirano, T. Kamiya, H. Hoaono, J. Lumin. 122–123 (2007) 339–341.
[19] S.S. Yao, L.H. Xue, Y.Y. Li, Y. You, Y.W. Yan, Appl. Phys. B 96 (2009) 39–42.
[20] H.A. Höppe, Angew. Chem. Int. Ed. 48 (2009) 3572–3582.
[21] S.S. Yao, Y.Y. Li, L.H. Xue, Y. You, Y.W. Yan, Cent. Eur. J. Phys. 7 (2009) 800–805.
[22] C.P.A. Santa, F.S. Teles, Spectra Lux Software v 2.0 Beta, Photo, Quânticao Nanodispositivos, Renami, 2003.
[23] A.S. Maia, R. Stefani, C.A. Kodaira, M.C.F.C. Felinto, E.E.S. Teotonio, H.F. Brito, Opt. Mater. 31 (2008) 440–444.
[24] J.H. Lin, G.X. Lu, J. Du, M.Z. Su, C.K. Loong, J.W. Richardson Jr., J. Phys. Chem. Sol. 60 (1999) 975–983.
[25] A.M. Pires, M.R. Davolos, Chem. Mater. 13 (2001) 21–27.
[26] R.D. Shannon, Acta Crystrallogr. A 32 (1976) 751–767.
[27] F. Liebau, Structural Chemistry of Silicates, Structure, Bonding and Classification, Springer-Verlag, Berlin, 1985.
[28] Z.P. Yang, G.W. Yang, S.L. Wang, J. Tian, X.N. Li, Q.L. Guo, G.S. Fu, Mater. Lett. 62 (2008) 1884–1886.
[29] G. Blasse, J. Solid State Chem. 62 (1986) 207–211.
[30] D.L. Dexter, J. Chem. Phys. 21 (1986) 836–850.
[31] L. Jiang, C.K. Chang, D.L. Mao, C.L. Feng, Mater. Sci. Eng. B 103 (2003) 271–275.
[32] L.G. Van Uitert, J. Electrochem. Soc. 114 (1967) 1048–1053.
[33] L. Ozawa, P.M. Jaffe, J. Electrochem. Soc. 118 (1971) 1678–1679.